#### **HYDROPHOBICITY**

# Charge transfer across C-H---O hydrogen bonds stabilizes oil droplets in water

Saranya Pullanchery<sup>1</sup>, Sergey Kulik<sup>1</sup>, Benjamin Rehl<sup>1</sup>, Ali Hassanali<sup>2</sup>\*, Sylvie Roke<sup>1,3,4</sup>\*

The hydrophobic-water interface plays a key role in biological interactions. However, both the hydrophobic-water interfacial molecular structure and the origin of the negative zeta potential of hydrophobic droplets in water are heavily contested. We report polarimetric vibrational sumfrequency scattering of the O-D and C-H stretch modes of 200-nanometer hexadecane oil droplets dispersed in water. An unusually broad spectral distribution (2550 to 2750 per centimeter) of interfacial water molecules that were not hydrogen bonded to other water molecules was observed, as well as a blue shift in the vibrational frequency of the interfacial hexadecane C-H stretch modes. Oil and water frequency shifts correlated with the negative electrostatic charge. Molecular dynamics simulations demonstrated that the unexpected strong charge-transfer interactions arose from interfacial C-H···O hydrogen bonds.

ydrophobicity represents a fundamental physical property that determines a variety of processes in aqueous media, such as protein folding, self-assembly, and aggregation (1, 2). Submicrometer-sized hydrophobic oil droplets or particles in water are an important model system for understanding how hydrophobicity works. However, both the charge and the structure of these interfaces are highly debated. Since the late 19th and early 20th century (3-6), hydrophobic nanodroplets and air/gas bubbles have been prepared and investigated. Early experiments (4, 5) reported the surprising observation that oil droplets or air bubbles in water exhibit a negative zeta ( $\zeta$ ) potential. The  $\zeta$  potential is interpreted as the electrostatic potential at the slip plane of the droplet (7), which is the plane that separates moving molecules from stationary ones. There are two main explanations for the negative charge on oil droplets. The earliest explanation invokes the adsorption of hydroxide (OH<sup>-</sup>) ions, because these are the only ionic sources of negative charge in neat water. However, the adsorption of OH has not been spectroscopically verified (5, 8, 9), and most theoretical studies have not found any thermodynamic stabilization for OH at hydrophobic interfaces (10, 11). OH is a small, nonpolarizable ion that prefers to be hydrated instead of being adsorbed at an interface. More recently, the negative charge was explained by a charge-transfer mechanism involving elec-

within molecules. Although the model of charge transfer suggests that water is key to the existence of the charge on oil droplets, the structure of this water next to oil is equally controversial. Water in contact with extended planar interfaces of nonpolar liquids or gases has been investigated by vibrational sum-frequency spectroscopy (13, 14), an inherently surface-specific spectroscopic technique. However, the spectra recorded from the hydrophobic-water interface vary substantially throughout the literature (see the supplementary materials, section S1 and fig. S1, for a summary of data and experiments). As a consequence, the structure of water next to a hydrophobic liquid material remains unknown. In the case of water in contact with oil droplets, only the structure of the oil has been investigated using vibrational

tron density that is present at the interface

because of an asymmetric hydrogen (H)-bond

distribution in the aqueous interfacial region

(6). This picture has recently been refined by

molecular dynamics (MD) simulations (12)

predicting explicit charge transfer between

water and oil molecules. Charge transfer

implies the transfer of charge between two

molecules, and electrostatic polarization is a

measure of the displacement of bound charge.

Although these two concepts are related, po-

larization is often assumed to be confined

Here, the structure of water in contact with hydrophobic droplets dispersed in water was unraveled and the source of the negative charge was investigated. The interfacial H-bond network of hexadecane droplets in water was measured using polarimetric vibrational sumfrequency scattering (SFS). Spectral peak ratios showed that the H-bonding network was

sum-frequency scattering (6, 15). The vibrational

spectrum of water in contact with oil droplets has been recorded only partially (9, 16),

with inconclusive results concerning the

H-bond network of water.

stronger at the oil-water interface than at the air-water interface. Furthermore, polarization analysis revealed a broad spectral region from ~2550 to ~2750 cm<sup>-1</sup>, which originated from interfacial water molecules that interacted with the oil phase. These spectral features and interactions between water and oil suggest charge transfer from water O atoms to the C-H groups in the oil. This charge transfer was spectroscopically confirmed by a blue shift in the C-H modes of the interfacial oil molecules. MD simulations confirmed this observation and revealed the presence of improper C-H...O H bonds between water and oil. We showed two distinct ways to inhibit the charge transfer from water to oil molecules. leading to a near-zero or positive  $\zeta$  potential. In both cases, the C-H frequency shifts of the oil phase were inverted. Thus, the charge transfer from interfacial water to oil molecules is the origin of the negative charge of bare oil droplets in water and is responsible for their stabilization.

### Results and Discussion Investigating the water structure at the interface of pure oil droplets

Nanodroplets of n-hexadecane (C16) with an average diameter of 200 nm were prepared in neat heavy water (D<sub>2</sub>O) using ultrasonication (see the supplementary materials, section S2 and fig. S2). The vibrational SFS (Fig. 1A) spectra of droplets were measured in the O-D and C-H stretch regions using both SSP [i.e., S-polarized sum frequency (SF), S-polarized visible, and P-polarized infrared (IR)1 and PPP polarization combinations. Because the IR beam passed through the liquid phase, it was absorbed by water when it had a frequency content that matched the O-D stretch modes. Therefore, when the IR pulse traveled through the sample cell (Fig. 1B), each droplet was probed by an IR pulse that had a different spectral shape and intensity, resulting in strongly modified SFS spectra (17). For this reason, it was long deemed impossible to measure the surface vibrational spectrum of water for particles dispersed in water. However, recently, we determined the appropriate lightmatter interactions that allowed us to devise a method to retrieve the true surface response  $(|\Gamma^{(2)}|^2)$  from the measured SF spectral intensity  $(I_{SF})$  (17). The procedure is described in the supplementary materials, section S2.  $\Gamma^{(2)}$ is the effective second-order particle susceptibility that describes the spectral interfacial response of droplets dispersed in solution and is proportional to the square root of the measured intensity (18-20) (see the supplementary materials, section S2).

The resulting  $|\Gamma^{(2)}|^2$  spectrum of 2 vol% hexadecane droplets in  $D_2O$  (Fig. 1C, blue trace) showed the vibrational response of the O–D stretch modes of water and thus revealed

<sup>&</sup>lt;sup>1</sup>Laboratory for Fundamental BioPhotonics, Institute of Bioengineering (IBI), School of Engineering (STI), École Polytechnique Fédérale de Lausanne (EPFL), CH-1015 Lausanne, Switzerland. <sup>2</sup>International Centre for Theoretical Physics, 34100 Trieste, Italy. <sup>3</sup>Institute of Materials Science and Engineering (IMX), School of Engineering (STI), École Polytechnique Fédérale de Lausanne (EPFL), CH-1015 Lausanne, Switzerland. <sup>4</sup>Lausanne Centre for Ultrafast Science, École Polytechnique Fédérale de Lausanne (EPFL), CH-1015 Lausanne, Switzerland.

<sup>\*</sup>Corresponding author. Email: sylvie.roke@epfl.ch (S.R.); ahassana@ictp.it (A.H.)

Fig. 1. Water structure at bare oil droplet surface. (A) Energy-level diagram of the SFS experiment involving simultaneous excitation with an infrared (IR) and visible (VIS) beams. (B) Sketch of the vibrational SFS experiment on oil droplets in water.  $\theta$  is the scattering angle, L is the optical path length, and the magnified sample cross section shows the attenuation of IR intensity as the beam travels through the sample. (C) SFS spectra of hexadecane droplets in D<sub>2</sub>O (blue) and reflection sum-frequency generation spectra of the planar D<sub>2</sub>O-air interface [red; (14, 21)]. The solid lines are guides to the eye. The dashed lines indicate the frequencies of low- and high-frequency Hbonded O-D peaks. The dotted lines refer to water molecules that are not H bonded to water. The spectra were recorded using the SSP polarization combination. The gray shaded region summarizes the result of this study that there is a broad distribution of non-water-Hbonded water molecules. (D) Ratio between the low-(2395 cm<sup>-1</sup>) and high-(2500 cm<sup>-1</sup>) frequency bands of the SF spectrum of the planar  $D_2O$ -air interface as a function of temperature (red markers) with a quadratic polynomial fit to a lower temperature range (red line) (21). The ratio at the oil droplet surface is shown in blue.

Α В VIS D<sub>2</sub>O at 5 x10 SSF Air/water Air/water interface Oil droplet in water Oil droplet interface 2395/2500 Peak ratio [2]2 0.8 0.6 260 300 2200 2300 2400 2500 2600 2700 2800 320 280 Temperature (K) IR Frequency, cm<sup>-1</sup>

the structure of the H-bond network around the hydrophobic oil droplet. The spectral SF intensity between 2200 and 2800 cm<sup>-1</sup> reported on water molecules that had an anisotropic structure induced by the hexadecane droplet interface. For comparison, Fig. 1C also shows the interfacial SF water spectrum of the extended planar air-water interface (red trace) (21). The SF spectra of Fig. 1C had two broad features around 2395 and 2500 cm<sup>-1</sup> in common (dashed lines), and a narrow peak at 2745 cm<sup>-1</sup> was only visible in the air-water SF spectrum. The O-D stretch frequency decreased with increasing H-bond strength. Therefore, the feature at  $2500~{\rm cm}^{^{-1}}\,{\rm reported}$  on water molecules that were more weakly H bonded to other water molecules than the ones that were attributed to the feature at 2395 cm<sup>-1</sup>. The peak at 2745 cm<sup>-1</sup> in the air-water spectrum originated from interfacial O-D groups that were not H bonded (22, 23). Both SF spectra contained similar 2395 and 2500 cm<sup>-1</sup> features (Fig. 1C, dashed lines), but they differed at higher wave numbers.

To gain insight into the relative H-bonding strength between the two interfaces, we examined the peak ratio of the 2395 and 2500 cm<sup>-1</sup> features. This ratio is temperature dependent when measured at the air-water interface (14, 21) and provides insight into the relative amount of stronger versus weaker H-bonded water (Fig. 1D). Lowering the temperature at

the air-water interface increased the peak ratio of the 2395 and 2500 cm<sup>-1</sup> modes (14, 21), indicating that the population of stronger H bonds increased over that of weaker H bonds (Fig. 1D, red data). The blue marker in Fig. 1D indicates the ratio found for water at the oil droplet interface, which was higher than that of the air-water interface of the same temperature. Extrapolating this temperature dependence, we determined that the H-bonding network at the oil droplet surface at room temperature (293 K) was equivalent to that of an air-water interface near the freezing point (277 K, the temperature at which bulk water has its highest density). This implied a more enhanced H-bonded network near the oilwater interface.

In addition to stronger H bonding, there was also a clear difference in the high-frequency side of the spectrum. The non-H-bonded O-D mode at 2745 cm<sup>-1</sup> was not detected at the oil droplet-water interface. Inspecting the water spectrum adjacent to the oil droplets, a broadening of the high-frequency side was seen (Fig. 1C. dotted line), which could represent a red shift and broadening of the sharp feature at 2745 cm<sup>-1</sup> in the air-water spectrum. Water molecules that were not H bonded to other water molecules (having so-called "free O-D" modes) should exhibit specific polarization dependences depending on the spatial symmetry of the mode. Their presence could therefore be detected even if they were not spectrally separated from other water molecules.

## Polarimetry to assess molecular structure and interactions

Vibrational modes of molecular groups with different symmetry properties have different polarization dependences on the interacting optical fields. A free water molecule exhibits C<sub>2v</sub> symmetry, yet if the two O-D groups of a water molecule are asymmetric because of H bonding or other interactions, then each O-D group has  $C_{\scriptscriptstyle \varpi_V}$  symmetry. The relative signal strength measured by different polarization combinations depends on molecular orientation and symmetry. As it turns out, the symmetry species of the water molecules can be approximated as symmetric C<sub>2v</sub> O-D stretch modes ( $C_{\mathrm{2v\text{-}ss}}$ ),  $C_{\scriptscriptstyle\varpi_{V}}$  O-D stretch modes, and asymmetric C<sub>2v</sub> stretch O-D stretch modes (C2v-as), despite the water structure being more complex than that (for a description of this analysis, see the supplementary materials, section S3 and fig. S5). Therefore, the polarization intensity ratios for interfacial vibrational modes with these different symmetries were calculated taking all possible molecular tilt angles into account.

The black line in Fig. 2A shows the frequency-dependent SSP/PPP intensity polarization ratio. The red, green, and blue bands in Fig. 2A represent the computed intensity ratios for the  $C_{2v\text{-}ss}$  modes, the  $C_{\text{\tiny cw}}$  O-D modes, and

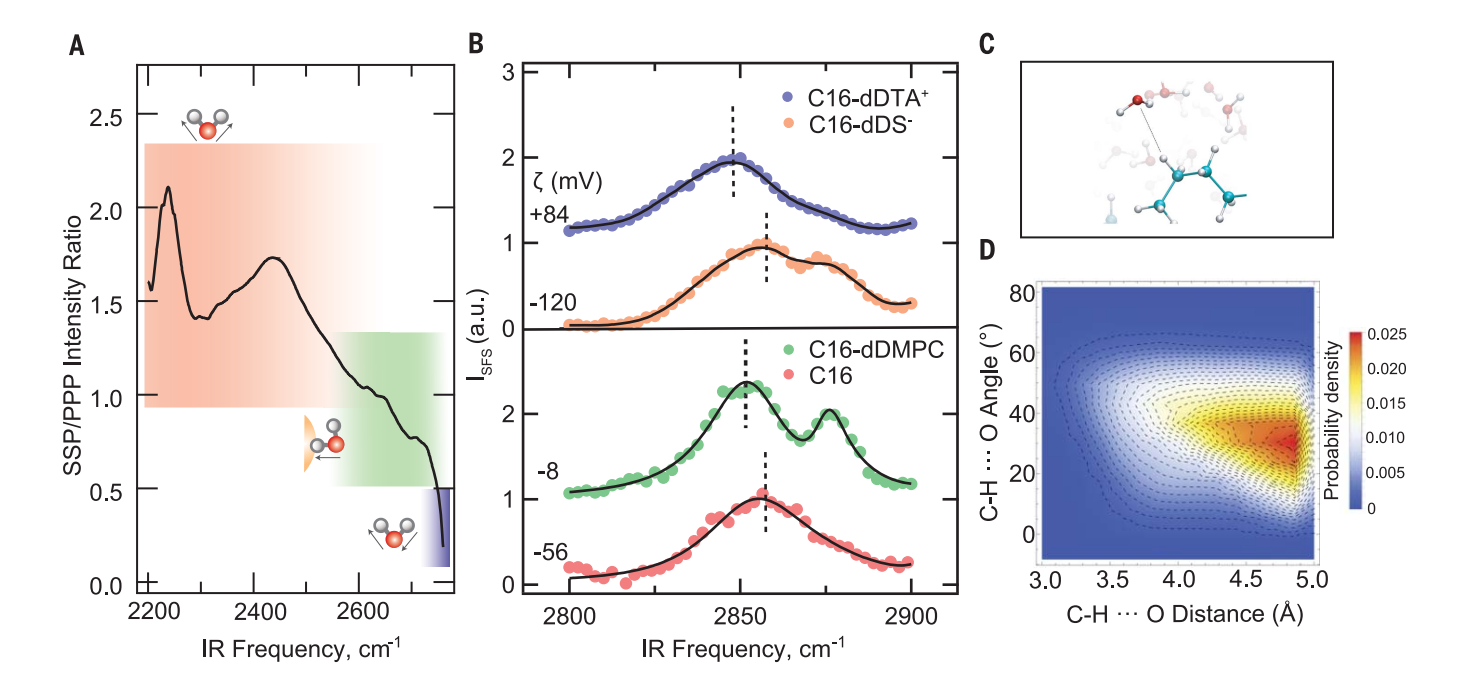


**Fig. 2. Interfacial C–H···O H bonds. (A)** SFS polarimetry. Shown is the SSP/PPP intensity ratio of the O–D spectrum as a function of IR frequency (black line). The shaded regions correspond to the calculated SSP–PPP intensity ratio of the  $C_{2v\text{-ss}}$  (red),  $C_{2v\text{-as}}$  (blue), and  $C_{\text{ov}}$  (green) modes. The frequency regions spanned by the calculated ratios were determined by comparison with the experimentally measured ratio. The vertical spread of the ratios was computed assuming any molecular orientation and takes into account a 10% uncertainty in the hyperpolarizability values, a scattering angle spread of 20°, and a droplet size distribution as described in the supplementary materials, section S3. **(B)** C–H peak shifts caused by charge transfer. The bottom panel contains the C–H spectra of bare hydrogenated oil droplets (C16, red) and hydrogenated oil droplets covered with d-DMPC (C16-dDMPC, green). The top

panel contains the C–H spectra of hydrogenated oil droplets covered with deuterated SDS (C16-dDS<sup>-</sup>, orange) and d-DTAB (C16-dDTA<sup>+</sup>, blue). The corresponding ζ-potential values are given next to each spectrum. All spectra were recorded using the SSP polarization combination. The solid black lines are smoothed data as guides to the eye. The dashed vertical lines represent the center frequency of the CH<sub>2</sub>-ss mode, implying the presence or absence of water-to-hexadecane charge transfer. (**C**) MD simulations showing C–H···O H bonds. A typical snapshot illustrates a C–H···O H-bonding–like configuration. (**D**) Two-dimensional probability density distribution associating the distance between the C atoms of oil (dodecane) and the O atoms of the water molecules nearby (*x* axis) with the corresponding angle between the C–H bond and the C–O bond vectors (*y* axis).

the C<sub>2v-as</sub> modes, respectively. Although the equations for computing the intensity ratios are different for scattering and reflection (24), the general selection rule that the SSP polarization combination generates a higher intensity than the PPP polarization combination for the C2v-ss modes was retained (25). The computed intensity ratios were compared with the measured ones to determine which frequency ranges reported primarily on which type of molecular symmetry. From Fig. 2A, we observed that the red band that reports on the C2v-ss mode spanned the largest frequency range of the measured data, from 2200 to 2550 cm<sup>-1</sup>. Additionally, the measured and computed intensity ratios from 2550 to 2745 cm<sup>-1</sup> agreed with the presence of  $C_{\omega v}$  O-D stretch modes. In the region where the red and the green bands overlapped, both modes were present. At frequencies higher than 2745 cm<sup>-1</sup>, the intensity ratios pointed to a small number of C<sub>2v-as</sub> modes. The high frequency of these water molecules suggested that there were no H-bonded water molecules to which H bonds could be donated. Because the SSP/PPP intensity ratio for this mode depended on the molecular orientation, we were able to determine that these water molecules were oriented with their O atom facing the oil (see the supplementary materials, section S4 and fig. S5). Furthermore, for the oil droplet interface, the frequency range of water molecules with  $C_{\rm ev}$  symmetry (i.e., lacking water–H bonds) was much broader (up to ~2550 to 2750 cm $^{-1}$ ). The center frequency of this range was at ~2650 cm $^{-1}$ , which was ~100 cm $^{-1}$  lower compared with the air–water interface. This red shift and broadening indicated an unexpected strong interaction between oil and water.

#### C-H---O H bonds

Generally, non-H-bonded O-D stretches appear as a sharp peak at ~2745 cm<sup>-1</sup> at the airwater interface (Fig. 1C). Raman hydration shell spectroscopy has reported significant broadening and red shifts of non-H-bonded water up to ~100 cm<sup>-1</sup> (26, 27). The sizable frequency shift of ~100 cm<sup>-1</sup> shown in Fig. 1C, highlighted by the gray peak shape, suggested that charge

must be transferred from the water O-D groups to the hexadecane C-H groups in the oil phase, because these were the only candidates for accepting electron density. If there were such a strong interaction, then we would expect that the vibrational modes of the oil molecules would experience a (blue) shift in the opposite direction as that of the high-frequency O-D modes (28, 29). These shifts should be accompanied by structural changes, such as the presence of C-H···O H bonds. To investigate this, the SFS spectra of interfacial C-H modes were recorded and MD simulations were performed.

Figure 2B (bottom panel) presents the SFS spectra of the interfacial C-H modes, showing both the symmetric CH<sub>2</sub> (CH<sub>2</sub>-ss) and CH<sub>3</sub> (CH<sub>3</sub>-ss) stretch modes around ~2850 and ~2878 cm<sup>-1</sup>, respectively. SFS spectra were recorded from the oil phase of bare oil droplets of hexadecane in water (Fig. 2B, red spectrum) and compared with oil droplets that were covered with a monolayer of deuterated 1,2-dimyristoyl-sn-glycero-3-phosphocholine (d-DMPC), a zwitterionic lipid (Fig. 2B, green

spectrum). The projected area of a single d-DMPC lipid within this monolayer was in the range of 0.65 to 0.75 nm<sup>2</sup> (see the supplementary materials, section S5). The CH2-ss mode occurred at 2851 cm<sup>-1</sup> for the d-DMPC-covered hexadecane droplets, whereas it occurred at 2856 cm<sup>-1</sup> for the bare oil droplets in water. A discussion of other spectral changes is given in the supplementary materials, section S5. The vibrational modes of the lipids were not at resonance in this spectral window. The spectral shift in the CH<sub>2</sub>-ss mode is highlighted by the vertical dashed lines in Fig. 2B. The CH2 modes of the oil directly in contact with D<sub>2</sub>O were clearly blue shifted, consistent with a transfer of negative charge from the water to the oil. This shift was not observed when d-DMPC was present because the full monolayer prevented the water from interacting with the oil.

To investigate the possible interactions that may emerge at the oil-water interface, MD simulations were performed for dodecanewater interfaces (see the supplementary materials, materials and methods). Figure 2C shows a typical snapshot of a dodecane-water interface in which the water and oil molecules interacted with one another, with the conformation reminiscent of an H bond between water and oil. In acting as an acceptor of a weak H bond from the C-H bond, the O lone pairs on water molecules donated some electron density, leaving the dodecane molecules with a negative charge. Figure 2D shows a twodimensional probability density distribution correlating the distances (x axis) and angular distributions (y axis) associated with possible H bonds that form between the water and the C-H groups of dodecane. The graph shows that a broad spectrum of interactions developed. Specifically, there was a significant population of water molecules in which the C-H bond vector pointed to the O lone-pair electrons in slightly distorted geometries (angle <20°) with larger distances (>~3.5 Å) than for waterwater H bonds. The water molecules that were within 5 Å from the oil phase oriented with their O atoms toward the CH<sub>2</sub> groups of the oil (see the supplementary materials, section S6 and fig. S6), in agreement with the polarimetric tilt angle analysis of the highfrequency water molecules (see the supplementary materials, section S4 and fig. S5). We thus concluded that C-H-O H bonds were responsible for the transfer of charge between water and oil and led to spectral shifts in both the interfacial water and interfacial oil molecules. C-H...O H bonds were discovered several decades ago (28) and were identified as being important structural factors in nucleic acid and protein structures, as well as in enzymatic reactions involving C-H groups and water molecules (30). To our knowledge, however, C-H--O H bonds have never been

associated with hydrophobicity or the interaction between water and oil, even though C-H modes of small molecules dissolved in water are known to display blue shifts in their C-H stretch frequencies (31). The blue shift in C-H modes arises from C-H bond contraction (28, 29). In H bonds in water, charge transfer is the primary contributor to all interactions, leading to bond lengthening and a red shift. C-H...O bonds have relatively weak charge transfer, and thus the Pauli repulsion between the filled C-H and O orbitals dominates the interactions (29), resulting in a blue shift (for details, see the supplementary materials, section S7). The charge transferred from water to oil was in the range of 0.025 to 0.05 electrons/ dodecane molecule (12). Although the energetic stabilization of single C-H···O H bonds is rather weak (a fraction of the thermal energy), the collective contribution of such small interactions can lead to a sufficient buildup of charge on the oil droplet, as predicted by Poli et al. (12).

# Oil-water charge-transfer interactions explain droplet stability

The oil droplets in this study had negative  $\zeta$ potential values of  $-56 \pm 10$  mV. Adding an insulating layer of d-DMPC lipids removed the frequency shift and the negative charge, reducing the  $\zeta$  potential to  $-8 \pm 6$  mV (32) (Fig. 2B, green). To further test whether the frequency shifts in the C-H modes were indeed correlated with the interfacial charge, hexadecane droplets with positively and negatively charged deuterated surfactants were prepared using d-dodecyltrimethylammonium bromide (d-DTA<sup>+</sup>) and d-sodium dodecyl sulfate (d-DS<sup>-</sup>), respectively. d-DS<sup>-</sup> and d-DTA<sup>+</sup> molecules formed dilute monolayers with a projected area per molecule of >4.25 nm<sup>2</sup> for d-DS<sup>-</sup> (33) and >5.00 nm<sup>2</sup> for d-DTA<sup>+</sup> (34) at their respective critical micelle concentrations. Adding d-DS up to the critical micelle concentration increased the magnitude of the  $\zeta$  potential further to -120  $\pm$  10 mV. The CH<sub>2</sub>-ss mode remained at 2856 cm<sup>-1</sup> (Fig. 2B, orange), because d-SD<sup>-</sup> adsorbed to the oil droplet surface in a dilute concentration without perturbing the oil molecules (15). Therefore, the absence of a blue shift in the CH2-ss frequency of d-DS--covered droplets compared with bare oil droplets indicated that adsorbed d-DSmolecules left enough oil-water contact points free to retain charge transfer. Adding positively charged d-DTA<sup>+</sup> up to the critical micelle concentration increased and inverted the sign of the  $\zeta$  potential to +84 ± 10 mV. d-DTA<sup>+</sup> adsorbed to the oil droplet surface in an equally diluted fashion as d-DS by inserting its alkyl tails and part of the head group into the oil phase (35), reverting the charge of the oil droplets to positive and thereby negating the charge transfer. Concomitantly, the CH2-ss mode frequency shifted to  $2847~{\rm cm}^{-1}$  (Fig. 2B, blue). Thus, reversal of charge also removed the blue shift observed for the bare oil droplet C–H modes. A possible molecular mechanism that relates charge transfer to negative  $\zeta$  potential is described in the supplementary materials, section S8 and fig. S7. The negation or retention of water-to-oil charge transfer in these droplet systems was correlated with their stability. Oil droplets covered with positively charged or neutral surfactants were significantly less stable than negatively charged droplets that retained the charge transfer on bare oil droplets (34).

#### Conclusions

In summary, interfacial water structure in contact with hydrophobic oil droplets was characterized by charge-transfer interactions between water and oil molecules that stem from improper C-H···O H bonds. Water at the oil droplet surface had a stronger H-bonding network compared with the planar air-water interface. The spectral shifts of interfacial O-D and C-H modes provided evidence for charge transfer from water to oil that explained the negative charge and stability of bare oil droplets in water.

#### **REFERENCES AND NOTES**

- D. Chandler, Nature 437, 640–647 (2005).
- P. Ball, Chem. Rev. **108**, 74–108 (2008).
- 3. J. K. Beattie, A. M. Djerdjev, *Angew. Chem. Int. Ed.* **43**, 3568–3571 (2004).
- 4. J. C. Carruthers, Trans. Faraday Soc. 34, 300-307 (1938).
- 5. N. Agmon et al., Chem. Rev. 116, 7642–7672 (2016).
- R. Vácha et al., J. Am. Chem. Soc. 133, 10204–10210 (2011).
- R. J. Hunter, Zeta Potential in Colloid Science: Principles and Applications (Academic Press, 1981).
- P. B. Petersen, R. J. Saykally, J. Phys. Chem. B 109, 7976–7980 (2005).
- J.-S. Samson, R. Scheu, N. Smolentsev, S. W. Rick, S. Roke, Chem. Phys. Lett. 615, 124–131 (2014).
- R. Vácha, V. Buch, A. Milet, J. P. Devlin, P. Jungwirth, Phys. Chem. Chem. Phys. 9, 4736–4747 (2007).
- Y.-L. S. Tse, C. Chen, G. E. Lindberg, R. Kumar, G. A. Voth, J. Am. Chem. Soc. 137, 12610–12616 (2015).
- 12. E. Poli, K. H. Jong, A. Hassanali, *Nat. Commun.* **11**, 901 (2020).
- L. F. Scatena, M. G. Brown, G. L. Richmond, Science 292, 908–912 (2001).
- S. Strazdaite, J. Versluis, E. H. G. Backus, H. J. Bakker, J. Chem. Phys. 140, 054711 (2014).
- H. B. de Aguiar, M. L. Strader, A. G. F. de Beer, S. Roke, J. Phys. Chem. B 115, 2970–2978 (2011).
- A. P. Carpenter, E. Tran, R. M. Altman, G. L. Richmond, Proc. Natl. Acad. Sci. U.S.A. 116, 9214–9219 (2019).
- S. Kulik, S. Pullanchery, S. Roke, *J. Phys. Chem. C* **124**, 23078–23085 (2020).
  S. Roke, M. Bonn, A. V. Petukhov, *Phys. Rev. B Condens. Matter*
- Mater. Phys. 70, 115106 (2004).
  A. G. F. de Beer, S. Roke, Phys. Rev. B Condens. Matter
- A. G. F. de Beer, S. Roke, Phys. Rev. B Condens. Matter Mater. Phys. **75**, 245438 (2007).
   J. I. Dadap, H. B. de Aguiar, S. Roke, J. Chem. Phys. **130**,
- 214710 (2009). 21. N. Smolentsev, W. J. Smit, H. J. Bakker, S. Roke, *Nat. Commun.*
- **8**, 15548 (2017). 22. Q. Du, R. Superfine, E. Freysz, Y. R. Shen, *Phys. Rev. Lett.* **70**,
- 23.13–23.16 (1993).
- 23. I. V. Stiopkin et al., Nature 474, 192–195 (2011).
- 24. A. G. F. de Beer, S. Roke, J. Chem. Phys. 132, 234702 (2010).
- H.-F. Wang, W. Gan, R. Lu, Y. Rao, B.-H. Wu, Int. Rev. Phys. Chem. 24, 191–256 (2005).

- J. G. Davis, K. P. Gierszal, P. Wang, D. Ben-Amotz, *Nature* 491, 582–585 (2012).
- 27. R. Scheu *et al.*, *Angew. Chem. Int. Ed.* **53**, 9560–9563 (2014).
- 28. P. Hobza, Z. Havlas, *Chem. Rev.* **100**, 4253–4264 (2000).
- Y. Mao, M. Head-Gordon, J. Phys. Chem. Lett. 10, 3899–3905 (2019).
- S. Horowitz, R. C. Trievel, J. Biol. Chem. 287, 41576–41582 (2012).
- D. S. Wilcox, B. M. Rankin, D. Ben-Amotz, Faraday Discuss. 167, 177–190 (2013).
- H. I. Okur, Y. Chen, N. Smolentsev, E. Zdrali, S. Roke, J. Phys. Chem. B 121, 2808–2813 (2017).
- 33. H. B. de Aguiar, A. G. F. de Beer, M. L. Strader, S. Roke, *J. Am. Chem. Soc.* **132**, 2122–2123 (2010).

- 34. E. Zdrali, Y. Chen, H. I. Okur, D. M. Wilkins, S. Roke, *ACS Nano* 11, 12111–12120 (2017).
- 35. R. Scheu *et al.*, *J. Am. Chem. Soc.* **136**, 2040–2047 (2014).
- S. Pullanchery, S. Kulik, B. Rehl, A. Hassanali, S. Roke, Data for: Charge transfer across C-H···O hydrogen bonds stabilizes oil droplets in water, Zenodo (2021); http://doi.org/10.5281/ zenodo.5549457.

#### **ACKNOWLEDGMENTS**

We thank H. Okur and H. B. de Aguiar for helpful discussions. S.R. thanks the Julia Jacobi Foundation. **Funding:** This work was supported by the Swiss National Science Foundation (grant 200021-182606-1 to S.P., S.K., B.R., and S.R.). **Author contributions:** S.P., S.K., and B.R. performed the experiments. S.P., S.R., S.K., B.R., and A.H. interpreted the data. A.H. performed

the simulations. S.R. conceived and supervised the study. S.R., S.P., A.H., B.R., and S.K. wrote the manuscript. **Competing interests:** The authors declare no competing interests. **Data and materials availability:** All data in the manuscript and supplementary materials are available through Zenodo (36).

#### SUPPLEMENTARY MATERIALS

science.org/doi/10.1126/science.abj3007 Materials and Methods Supplementary Text Figs. S1 to S7 Table S1 References (37–60)

4 May 2021; accepted 19 October 2021 10.1126/science.abj3007



## Charge transfer across C-H###O hydrogen bonds stabilizes oil droplets in water

Saranya PullancherySergey KulikBenjamin RehlAli HassanaliSylvie Roke

Science, 374 (6573), • DOI: 10.1126/science.abj3007

#### Why oil and water do not mix

It is well known that oil forms stable droplets that carry a negative electrophoretic mobility (and negative charge) upon dispersing in water. However, the underlying mechanism is a long-debated topic. Using vibrational sum-frequency scattering spectroscopy, Pullanchery et al. recorded the interfacial vibrational spectrum in the oxygen-deuterium and carbon-hydrogen stretching regions of a hexadecane-water interface. Their spectral analysis accompanied by molecular dynamics simulations showed that water molecules form "improper" interfacial hydrogen bonds with alkyl hydrogens, resulting in the water-to-oil charge transfer that stabilizes oil droplets. This work demonstrates that sum-frequency scattering spectroscopy is a powerful technique that can improve our understanding of hydrophobicity in water-mediated chemical and biological systems. —YS

#### View the article online

https://www.science.org/doi/10.1126/science.abj3007 **Permissions** 

https://www.science.org/help/reprints-and-permissions

Use of think article is subject to the Terms of service